

# Effect of $\text{Na}_2\text{S}_2\text{O}_3 \cdot 5\text{H}_2\text{O}$ concentration on the properties of $\text{Cu}_2\text{ZnSn}(\text{S}, \text{Se})_4$ thin films fabricated by selenization of co-electroplated Cu-Zn-Sn-S precursors

GE Jie<sup>1,2</sup>, JIANG Jin-Chun<sup>1,2\*</sup>, HU Gu-Jin<sup>2,3</sup>, ZHANG Xiao-Long<sup>1</sup>, ZUO Shao-Hua<sup>2</sup>, YANG Li-Hong<sup>2</sup>, MA Jian-Hua<sup>2,3</sup>, CAO Meng<sup>3</sup>, YANG Ping-Xiong<sup>1</sup>, CHU Jun-Hao<sup>1,2,3</sup>

- (1. Key Laboratory of Polar Materials and Devices, Department of Electronic Engineering, East China Normal University, Shanghai 200241, China
2. Shanghai Center for Photovoltaics, Shanghai 201201, China
3. National Laboratory for Infrared Physics, Shanghai Institute of Technical Physics, Chinese Academy of Sciences, Shanghai 200083, China)

**Abstract:**  $\text{Cu}_2\text{ZnSn}(\text{S}, \text{Se})_4$  films were fabricated through post-selenization of Cu-Zn-Sn-S precursors co-electroplated by varied  $\text{Na}_2\text{S}_2\text{O}_3 \cdot 5\text{H}_2\text{O}$  concentrations. The property of obtained films before and after selenization shows a close dependence on the concentration of  $\text{Na}_2\text{S}_2\text{O}_3 \cdot 5\text{H}_2\text{O}$ . Only the film grown by 5 mM of  $\text{Na}_2\text{S}_2\text{O}_3 \cdot 5\text{H}_2\text{O}$  shows a uniform surface with faceted grains, a Zn-poor composition, a single phased  $\text{Cu}_2\text{ZnSn}(\text{S}, \text{Se})_4$  structure and a 1.11 eV band gap evidencing by SEM, EDS, XRD, Raman and transmittance spectra. More than 5 mM of  $\text{Na}_2\text{S}_2\text{O}_3 \cdot 5\text{H}_2\text{O}$  additive to the electrolyte yielded the films with rougher morphology and the presence of  $\text{SnSe}_x$ . Less than 5 mM of  $\text{Na}_2\text{S}_2\text{O}_3 \cdot 5\text{H}_2\text{O}$  additive to the electrolyte resulted in the films with highly Zn-poor content and the primary formation of  $\text{Cu}_2\text{SnSe}_3$ .

**Key words:**  $\text{Cu}_2\text{ZnSn}(\text{S}, \text{Se})_4$  thin film,  $\text{Na}_2\text{S}_2\text{O}_3 \cdot 5\text{H}_2\text{O}$  concentration, co-electroplating, selenization

**PACS:** 68.55.-a, 81.15.Pq, 84.60.Jt

## 硫代硫酸钠浓度对电沉积制备铜锌锡硫硒薄膜性质的影响

葛杰<sup>1,2</sup>, 江锦春<sup>1,2\*</sup>, 胡古今<sup>2,3</sup>, 张小龙<sup>1</sup>, 左少华<sup>2</sup>,  
杨立红<sup>2</sup>, 马建华<sup>2,3</sup>, 曹萌<sup>3</sup>, 杨平雄<sup>1</sup>, 褚君浩<sup>1,2,3</sup>

- (1. 华东师范大学 电子工程系 极化材料与器件教育部重点实验室, 上海 200241;
2. 上海太阳能电池研究与发展中心, 上海 201201;
3. 中国科学院上海技术物理研究所 红外物理国家重点实验室, 上海 200083)

**摘要:** 采用后硒化 Cu-Zn-Sn-S 电沉积预制层的方法制备了铜锌锡硫硒薄膜, 其中 Cu-Zn-Sn-S 预制层是通过含有不同浓度的硫代硫酸钠电解液电沉积而成的. 实验发现, 硒化前后薄膜的性质与硫代硫酸钠浓度密切相关. SEM, EDS, XRD, Raman 和透射光谱分析表明, 当硫代硫酸钠的浓度为 5 mM 时, 沉积的薄膜形貌平整, 晶粒明显, 组分贫锌, 具有单一的铜锌锡硫硒结构, 且其带隙为 1.11 eV; 在浓度高于 5 mM 下沉积的薄膜形貌粗糙并产生杂相硒化锡; 在浓度低于 5 mM 下沉积的薄膜组分严重贫锌并生成大量的  $\text{Cu}_2\text{SnSe}_3$ .

**关键词:** 共电沉积; 硫代硫酸钠浓度; 硒化; 铜锌锡硫硒薄膜

中图分类号: TM914.4 文献标识码: A

Received date: 2012-08-24, revised date: 2013-04-02

收稿日期: 2012-08-24, 修回日期: 2013-04-02

**Foundation items:** Supported by National Natural Science Foundation of China (11174307, 11074265, 61006092, 61006089), Science and Technology Commission of Shanghai Municipality (10JC1414300, 10JC1404600), and Knowledge Innovation Program of the Chinese Academy of Sciences (Y2K4401DG0)

**Biography:** GE Jie (1985-), male, Kaifeng, Henan, PhD candidate. Research involves solar materials and solar cells. E-mail: ge-jie@ecnu.cn

\* **Corresponding author:** E-mail: jchang2007@hotmail.com

## Introduction

$\text{Cu}_2\text{ZnSnS}_4$  (CZTS), a p-type semiconductor for solar cell applications, is made entirely of abundant materials and has a high absorption coefficient. The advantages merit the possible replacement for Cu (In, Ga)Se<sub>2</sub> (CIGS) thin film solar cells. Due to the possibility to tune the band gap by the introduction of isovalent atoms with different size, the band gap of CZTS can be decreased by substituting Se atoms for smaller S atoms by post-deposition selenization. The ability to tailor the band gap therefore enables tuning the absorption characteristics over the spectral range of interest for the solar spectrum. Changes in the band gap can also yield higher short current density per cell – advantageous for large-area modules because of reduced series resistance losses. Until recently, 10.1% power conversion efficiency has been achieved for the  $\text{Cu}_2\text{ZnSn}(\text{S},\text{Se})_4$  (CZTSSe, [S/Se]  $\approx$  0.4) solar device using a hydrazine-based solution via spin coating<sup>[1]</sup>.

Since these compounds were proposed by Friedlmeier et al<sup>[2]</sup>. in 1997, by far various synthesis approaches have been implemented, including thermal evaporation<sup>[3]</sup>, sputtering<sup>[4]</sup>, ink-based approach<sup>[5]</sup>, etc. Among these approaches, electroplating is a promising non-vacuum chemical method for the large-area production pilot of thin film solar cells, since electroplating of copper, zinc, tin and their alloys are very common and mature for the commercial application in printed circuit boards, semiconductor chips, decorative coatings, etc. The elemental layers Zn/Sn/Cu/Mo were sequentially electroplated one-by-one to form a stacked precursor, leading to a 3.2% efficient CZTS solar cell after sulfurization<sup>[6]</sup>. Via a selenization or sulfurization of co-electroplated Cu-Zn-Sn alloy route, solar devices with 1.7% efficiency for pure CZTSe and 3.16% for pure CZTS have been achieved<sup>[7-8]</sup>, and the electrolytes involved  $\text{CuSO}_4$ ,  $\text{ZnSO}_4$ , and  $\text{SnSO}_4$  as well as  $\text{Na}_3\text{C}_6\text{H}_5\text{O}_7$  as complexing agent. Kim et al additionally added  $\text{Na}_2\text{S}_2\text{O}_3$  (sulfur source) into the aforementioned electrolytic bath and consequently the metals as well as adequate sulfur were co-electroplated<sup>[9]</sup>. No post-sulfurization was required, with the

precursors being annealed in argon. They additionally studied the effect of complexing agent  $\text{Na}_3\text{C}_6\text{H}_5\text{O}_7$ <sup>[10]</sup>, none the less no solar cell device results has yet been reported using this method. On the other hand, it is seldom reported the fabrication of CZTSSe alloy films via selenization of electroplated precursors.

In this study, we fabricated several CZTSSe films on ITO glasses, for the bifacial device<sup>[11]</sup>, by post-selenization of co-electroplated Cu-Zn-Sn-S precursors under varied  $\text{Na}_2\text{S}_2\text{O}_3$  concentrations, and the role of  $\text{Na}_2\text{S}_2\text{O}_3$  during the co-electroplating was discussed.

## 1 Experiment

Co-electroplating of Cu-Zn-Sn-S precursors was performed in a potentiostatic condition with a CHI 1140 A electrochemical workstation (CH Instrument, USA) in a three-electrode system. The reference electrode was Ag/AgCl and a platinum foil served as the counter electrode. The working electrodes were ITO glass substrates (2 cm  $\times$  3 cm) which had been cleaned ultrasonically in acetone, ethanol and deionized water and dried under flowing nitrogen. The aqueous electrolyte contained  $\text{CuSO}_4 \cdot 5\text{H}_2\text{O}$ ,  $\text{ZnSO}_4 \cdot 7\text{H}_2\text{O}$ ,  $\text{SnSO}_4$  and  $\text{Na}_2\text{S}_2\text{O}_3 \cdot 5\text{H}_2\text{O}$  as well as  $\text{Na}_3\text{C}_6\text{H}_5\text{O}_7$  and  $\text{C}_4\text{H}_4\text{K}_2\text{O}_6$  as complexing agents. All the chemicals were analytical reagent grade (Sinopharm Chemical Reagent Co. Ltd. China). Only the concentration of  $\text{Na}_2\text{S}_2\text{O}_3 \cdot 5\text{H}_2\text{O}$  was varied from 1 mM to 9mM at an interval of 2 mM. The precursors were deposited under a constant potential of -1.15 V for 15min at room temperature without stirring. After deposition, the samples were rinsed using deionized water and dried under flowing nitrogen. Those as-deposited precursors were selenized simultaneously at a graphite box placed into a tubular furnace at 550°C for 40min. This graphite box is artfully designed as the selenization reaction container, in which Se powder together with the precursors are heated simultaneously<sup>[11]</sup>. The usage amount of Se powder was 0.7 g and the pressure in the furnace was kept at 18 Torr.

The structural property of CZTSSe thin films was analyzed by X-ray diffraction (XRD) using Bruker D8 diffractometer with Cu  $K_\alpha$  radiation ( $\lambda = 0.15418$  nm). Surface morphology was studied using a Phil-

ipsS360 scanning electron microscope (SEM). The chemical composition of the samples was determined by an energy dispersive X-ray spectroscopy (EDS) system. The optical properties were measured with the help of a Cary-5000 UV-Vis-NIR double-beam spectrophotometer in the wavelength range 300 ~ 1500 nm. The thickness was obtained using a DEKTAK profilometer. The CZTSSe films were additionally analyzed by Raman spectroscopy (Jobin Yvon LabRAM HR 800 UV MicroPL, a 488 nm laser).

## 2 Results and discussion

Figure 1 shows the morphologic images of these CZTSSe films before and after selenization. As clearly seen, all these precursors present a surface comprising of ball-like particles with different sizes. More  $\text{Na}_2\text{S}_2\text{O}_3 \cdot 5\text{H}_2\text{O}$  additive to the electrolyte has given rise to the rougher surface morphologies of the precursors (see Fig. 1 (e)-(a)) and yielded the overgrown cauliflower-like particles located on the surface (see Fig. 1(a)). After selenization, only the film grown by 5 mM of  $\text{Na}_2\text{S}_2\text{O}_3 \cdot 5\text{H}_2\text{O}$  presents a compact and uniform surface with faceted grains (Fig. 1 (C)). The selenized films processed with 1 mM of  $\text{Na}_2\text{S}_2\text{O}_3 \cdot 5\text{H}_2\text{O}$  present discontinuous surfaces (Fig. 1 (E)), for which the evaporation of Sn via SnSe and heavily Zn-poor content to be revealed below should be responsible. In addition, the films grown by 7 mM and 9 mM of  $\text{Na}_2\text{S}_2\text{O}_3 \cdot 5\text{H}_2\text{O}$  after selenization show similar morphological surfaces full with giant agglomerates (Figs. 1(B) and (A)). EDS has proved these regions are Sn rich and highly Se rich, suggesting the formation of agglomerates of tin selenide and selenium phases. The big particles on film top shown in Fig. 1 (a) and (b) may absorb excess Se vapor and possibly give rise to the presence of big agglomerates on the film top after selenization.

Table 1 lists the composition of the films grown with different concentrations of  $\text{Na}_2\text{S}_2\text{O}_3 \cdot 5\text{H}_2\text{O}$  before and after selenization. As clearly can be seen, all these films show the Zn-poor composition, indicating the Zn is hard to be reduced at the cathode for the more negative deposition potential. As the concentration of  $\text{Na}_2\text{S}_2\text{O}_3 \cdot 5\text{H}_2\text{O}$  was increased in the electro-

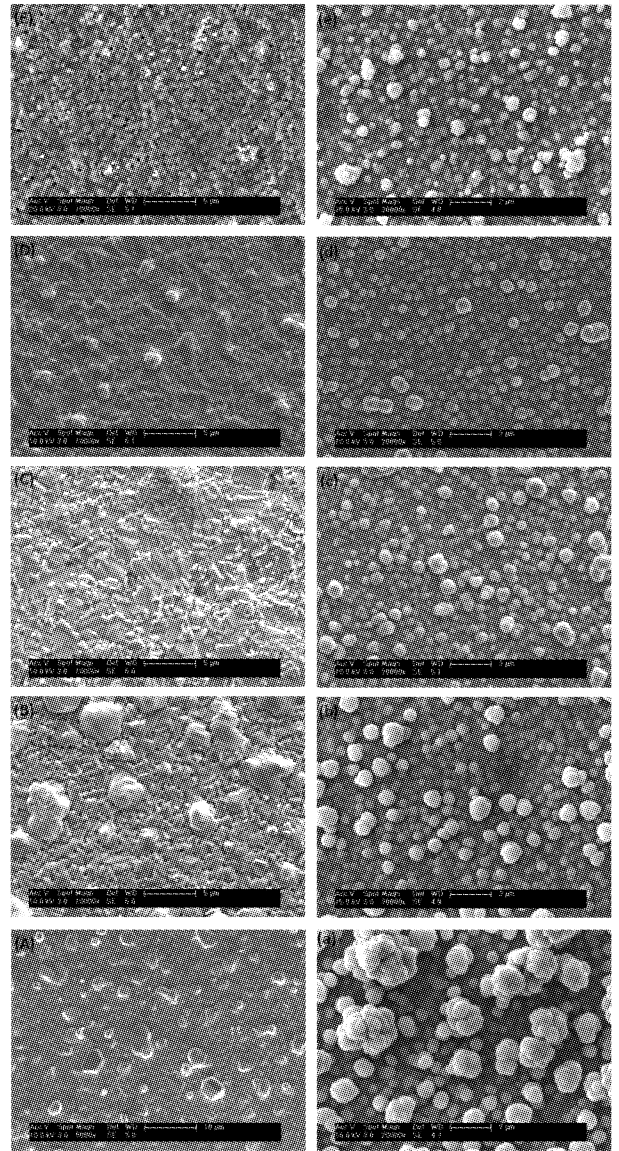


Fig.1 SEM of the CZTSSe films deposited with different concentrations of  $\text{Na}_2\text{S}_2\text{O}_3 \cdot 5\text{H}_2\text{O}$  before and after selenization. (A) 9 mM, (B) 7 mM, (C) 5 mM, (D) 3 mM, and (E) 1 mM are the SEM images of the films after selenization. (a) - (e) are the SEM images of the corresponding precursors  
图1 不同硫代硫酸钠浓度下沉积的 CZTSSe 薄膜 [(A) 9mM, (B) 7 mM, (C) 5 mM, (D) 3 mM, and (E) 1 mM] 及其前躯体 [(a) - (e)] 的形貌图

lyte, both the Zn and S percentages of the precursors show a slight increasing trend, whereas, the percentages of Cu and Sn of the precursors decreases. It is hard to give a clear explanation for the role of  $\text{Na}_2\text{S}_2\text{O}_3 \cdot 5\text{H}_2\text{O}$  since the co-electroplating is a relatively complicated process. Comparing the [Cu/Sn] ratio before and after selenization, we find that the films after selenization should have a desired ratio of [Cu/Sn] close

to 2.0, because the excess Sn in the precursors has been ruled out via the volatile SnSe. On the other hand, the selenized films wholly show a more or less Se-rich content. The excess Se in the films possibly forms the Se agglomerates on the surface (Figs. 1 (A), (B) and (D)) or dissolves into the films in terms of interstitials, the presence of which will affect the electrical properties of the films<sup>[12]</sup>. Although much excessive Se has been absorbed, S atom has still not been replaced completely by Se atom after selenization, which is quite consistent with the reported works<sup>[11]</sup>.

**Table 1** Compositional results of the CZTSSe films deposited with different concentrations of  $\text{Na}_2\text{S}_2\text{O}_3 \cdot 5\text{H}_2\text{O}$  before and after selenization

**表 1** 不同硫代硫酸钠浓度下沉积的 CZTSSe 薄膜及其前驱体的组分

mM	Before selenization (%)					After selenization (%)						
	Cu	Zn	Sn	S	Cu/Sn	Cu	Zn	Sn	S	Se	Cu/Sn	S+Se/Me
1	45.3	3.2	41.9	9.6	1.1	27.4	1.9	13.3	1.0	56.3	2.1	1.3
3	45.4	6.7	37.6	10.3	1.2	17.1	6.3	10.9	4.9	61.8	1.6	1.9
5	39.8	18.7	24.4	17.2	1.5	22.1	8.5	13.3	6.0	50.1	1.7	1.3
7	33.7	15.4	29.1	24.8	1.2	18.8	7.3	9.6	4.4	59.9	1.9	1.8
9	34.8	15.3	25.8	24.2	1.3	18.8	7.5	10.9	5.1	56.6	1.7	1.7

Raman scattering can be used to characterize CZTSe reliably, because identification of the phases, ZnSe (F-43 m JCPDS 88-2345) and  $\text{Cu}_2\text{SnSe}_3$  (F-43 m JCPDS 89-2879) which have similar symmetries and lattice parameters with CZTSe, is challenging by XRD. Fig. 2 depicts the Raman spectra for these selenized films grown by different concentrations of  $\text{Na}_2\text{S}_2\text{O}_3 \cdot 5\text{H}_2\text{O}$ . Only the film grown by 5mM of  $\text{Na}_2\text{S}_2\text{O}_3 \cdot 5\text{H}_2\text{O}$  presents the Raman peaks that can be assigned as the characteristic modes of stoichiometric CZTSe<sup>[11]</sup>, which confirms that the film presents the kesterite/stannite structure with a Zn-poor content. On the other hand, the selenized films grown by 1 mM and 3 mM of  $\text{Na}_2\text{S}_2\text{O}_3 \cdot 5\text{H}_2\text{O}$  present the intense Raman vibrations at  $182 \text{ cm}^{-1}$ ,  $231 \text{ cm}^{-1}$ , and  $253 \text{ cm}^{-1}$  originating from  $\text{Cu}_2\text{SnSe}_3$  phase<sup>[13]</sup>, indicating a quite small Zn content in the films. The films grown with 7 mM and 9 mM of  $\text{Na}_2\text{S}_2\text{O}_3 \cdot 5\text{H}_2\text{O}$  show the intense Raman peak arising from tin selenide phases at  $186 \text{ cm}^{-1}$ <sup>[14]</sup>, as well as a wide vibrational peak from Se-Se from 230

$\text{cm}^{-1}$  to  $260 \text{ cm}^{-1}$ <sup>[15]</sup>, which indicates that the film surfaces are full with these spurious phases. The 488nm laser failed to detect CZTSSe phase beneath the films due to the small penetration depth.

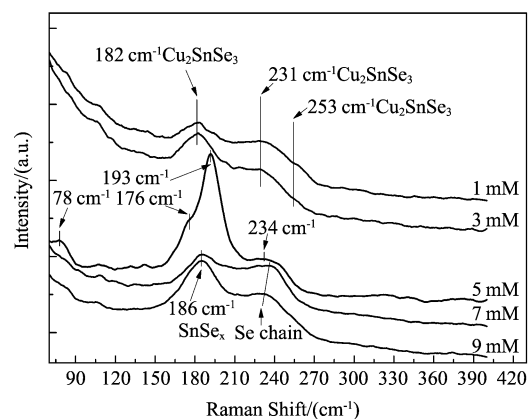


**Fig. 2** Raman spectra of the selenized CZTSSe films deposited with different concentrations of  $\text{Na}_2\text{S}_2\text{O}_3 \cdot 5\text{H}_2\text{O}$   
图 2 不同硫代硫酸钠浓度下沉积的 CZTSSe 薄膜的拉曼散射图

Figure 3 plots the XRD data of these selenized films processed with different concentrations of  $\text{Na}_2\text{S}_2\text{O}_3 \cdot 5\text{H}_2\text{O}$ . Due to the lower symmetry, CZTSe shows additional minor peaks (101, 103, 121 etc.) that are not in the patterns of ZnSe or  $\text{Cu}_2\text{SnSe}_3$ . However, there is no trace of these minor Bragg peaks 101, 121 or 103 in the XRD patterns of the films grown by 1mM of  $\text{Na}_2\text{S}_2\text{O}_3 \cdot 5\text{H}_2\text{O}$ , indicating the percentage of Zn is quite so little that  $\text{Cu}_2\text{SnSe}_3$  is predominantly present in the films. As the Zn concentration increases up to 6.3%, 101, 121 and 103 minor peaks are clearly observed in the XRD patterns. Thus, the presence of CZTSSe can be confirmed in the films grown by 3mM-9mM of  $\text{Na}_2\text{S}_2\text{O}_3 \cdot 5\text{H}_2\text{O}$ . As additionally can be seen in Fig. 3 (a), the trace of  $\text{SnSe}_x$  has been confirmed in the films processed with 7 mM and 9 mM of  $\text{Na}_2\text{S}_2\text{O}_3 \cdot 5\text{H}_2\text{O}$  evidencing by the intense peaks at  $30.140^\circ$  and  $31.282^\circ$  based on JCPDS 32 ~ 1382. Besides, the peaks arising from the crystallized ITO glass have been found. Peaks at  $33.737^\circ$ ,  $37.800^\circ$ ,  $51.602^\circ$  and  $54.538^\circ$  are the intense directions of  $\text{SnO}_2$  (JCPDS 77-0452). Peaks at  $30.263^\circ$ ,  $35.264^\circ$ , and  $50.661^\circ$  should be the major peaks of  $\text{In}_2\text{O}_3$  (JCPDS 06-0416). Similar XRD peaks of ITO

substrates have been reported elsewhere<sup>[11, 16]</sup>. Moreover, given no relative diffraction peak was detected by XRD in Fig. 3(a) for the film grown by 0.7 g Se powder, it was assumed that the excessive Se possibly dissolved in CZTSSe films in an amorphous state.

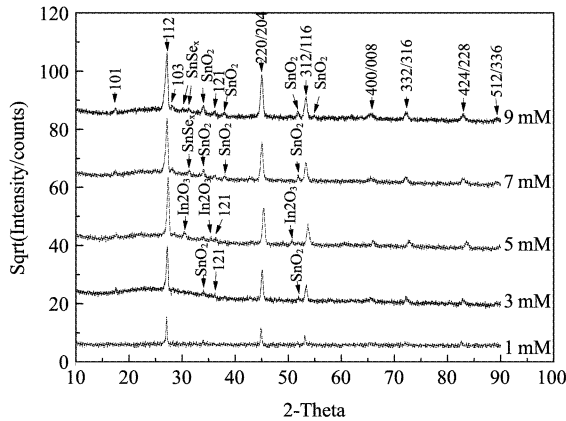


Fig. 3 XRD patterns of CZTSSe films after selenization deposited with different concentrations of  $\text{Na}_2\text{S}_2\text{O}_3 \cdot 5\text{H}_2\text{O}$

图3 不同硫代硫酸钠浓度下沉积的 CZTSSe 薄膜的 XRD 图

Since the band gap of CZTSSe is direct and occurs at the  $\Gamma$  point, its optical band gap can be deduced from the expression,  $(\alpha hv)^2 \propto (hv - E_g)$ , where  $E_g$  is the band gap energy and  $h\nu$  is the photon energy. The absorption coefficient  $\alpha$  was determined by  $\alpha = [-\ln(T)]/t$ , where  $t$  is the required thickness of the layers. Fig. 4 plots the band gap estimated from the curves of  $(\alpha hv)^2$  vs.  $h\nu$ . Band gap values were given by extrapolating the straight line portion of the graph in the high absorption regime. The corresponding values of band gap for each sample are shown in the inset. As can be seen, all the band gap values vary from 0.91 eV to 1.11 eV around that of the purely stoichiometric CZTSe (0.96 eV). 0.91 eV for the sample grown with 1 mM of  $\text{Na}_2\text{S}_2\text{O}_3 \cdot 5\text{H}_2\text{O}$  is slightly bigger than the band gap 0.84 eV of  $\text{Cu}_2\text{SnSe}_3$ <sup>[12]</sup>, possibly due to the slight incorporation of Zn and S into the film.

### 3 Conclusions

In this work, we electro-chemically deposited a set of Zn-poor CZTSSe films with different concentrations of  $\text{Na}_2\text{S}_2\text{O}_3 \cdot 5\text{H}_2\text{O}$ .  $\text{Na}_2\text{S}_2\text{O}_3 \cdot 5\text{H}_2\text{O}$  can affect Zn content and surface morphology of the metallic prec-

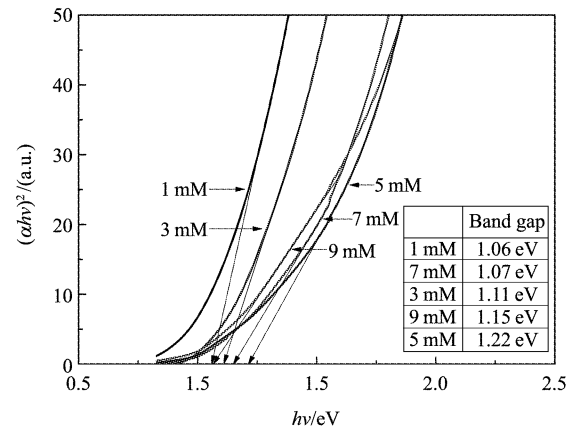


Fig. 4 Optical band gap estimation for the selenized CZTSSe films deposited with different concentrations of  $\text{Na}_2\text{S}_2\text{O}_3 \cdot 5\text{H}_2\text{O}$ .

图4 不同硫代硫酸钠浓度下沉积的 CZTSSe 薄膜的光学带隙估算图

ursors. Zn is seldom reduced at the cathode when the usage amounts of  $\text{Na}_2\text{S}_2\text{O}_3 \cdot 5\text{H}_2\text{O}$  is too small (below 3 mM). As more  $\text{Na}_2\text{S}_2\text{O}_3 \cdot 5\text{H}_2\text{O}$  is added, the precursors present rougher surfaces and a slightly increased Zn content. The kesterite/stannite structure has been clearly observed by XRD when the Zn percentage in the selenized film was attained at 6.3%. The selenized film grown with 5 mM of  $\text{Na}_2\text{S}_2\text{O}_3 \cdot 5\text{H}_2\text{O}$  shows single phase CZTSSe structure, a uniform surface with facet grains and a Zn-poor and Sn-rich content. More importantly, it shows the similar properties with stoichiometric CZTSSe films evidencing by Raman, XRD and transmittance spectrum analyses. For the photovoltaic CZTSSe absorber, the composition should be Zn-rich. Thus, the electrolyte must be improved in the future.

### REFERENCES

- [1] Barkhouse D A R, Gunawan O, Gokmen T, *et al.* Device characteristics of a 10.1% hydrazine-processed  $\text{Cu}_2\text{ZnSn}(\text{Se}, \text{S})_4$  solar cell [J]. *Prog. Photovolt: Res. Appl.*, 2012, **20** (1): 6–11.
- [2] Friedlmeier T M, Dittrich H, Schock H W. Growth and characterization of  $\text{Cu}_2\text{ZnSnS}_4$  and  $\text{Cu}_2\text{ZnSnSe}_4$  thin films for photovoltaic applications [J]. *ICTMC-11*, 1997: 345–348.
- [3] Bhaskar P U, Babu G S, Kumar Y B K, *et al.* Investigations on co-evaporated  $\text{Cu}_2\text{SnSe}_3$  and  $\text{Cu}_2\text{SnSe}_3 - \text{ZnSe}$  thin films [J]. *Appl. Surf. Sci.*, 2011, **257** (20): 8529–8534.

(下转第 303 页)

390℃三种温度下退火的形貌、结构和光学性能,得出:在干燥空气中退火,CdS 薄膜晶体质量明显改善,同时晶粒度和表面粗糙度增大不明显,可见光透过率和吸收系数没有显著影响;在 CdCl<sub>2</sub> 源 + 干燥空气中退火,CdCl<sub>2</sub> 显著降低了 CdS 薄膜的再结晶温度,促进再结晶和晶粒长大,随着退火温度的升高,晶粒大小分布不均匀性和表面粗糙度增大,390℃退火表面粗糙度最高为 34.83 nm,可见光透过率随退火温度的升高而下降。退火明显增大了溅射 CdS 薄膜的光学带隙  $E_g$ ,在干燥空气中退火, $E_g$  随退火温度的升高而增大,在 CdCl<sub>2</sub> 源 + 干燥空气中退火, $E_g$  随退火温度的升高而减小,是退火引起带尾态有效掺杂浓度变化的结果。

根据实验结果判断,对于上层配置的 CdTe 薄膜太阳能电池,在 CdCl<sub>2</sub> 源 + 干燥空气中退火,温度不宜超过 390℃。对于下层配置的 CdTe 薄膜太阳能电池,CdS 薄膜窗口层适宜在干燥空气中退火,对退火温度的选取除参考本文结果外,还需考虑退火引起 CdS/CdTe 界面层的元素扩散等因素进一步研究确定。

## REFERENCES

- [1] Tsuji M, Aramoto T, Ohyama H, *et al.* Characterization of CdS thin film in high efficient CdS/CdTe solar cells [J]. *Journal of Crystal Growth*, 2000, 214 - 215: 1142 - 1147.
- [2] Repins I, Glynn S, Duenow J, *et al.* Required materials properties for high-efficiency CIGS modules [R], NREL/CP-520-46235, presented at the Society of Photographic Instrumentation Engineers (SPIE) 2009 Solar Energy + Technology Conference. San Diego, California; August 2 - 6, 2009.
- [3] Vasko A C. All-sputtered CdS/CdTe solar cells on polyimide [C], 2009. proceeding of the 34th IEEE Photovoltaic Specialists Conference (PVSC), Philadelphia, Pennsylvania USA, June 7-12, 2009, p: 001552 - 001555.
- [4] Hernández-Contreras J, Contreras-Puente G, Aguilar-Hernández J, *et al.* CdS and CdTe large area thin films processed by radio-frequency planarmagnetron sputtering [J], *Thin Solid Films*, 2002, 403 - 404: 148 - 152.
- [5] Lee J H, Lee D J. Effects of CdCl<sub>2</sub> treatment on the properties of CdS films prepared by r. f. magnetron sputtering [J], *Thin Solid Films*, 2007, 515: 6055 - 6059.
- [6] Moon B S, Lee J H, Jung H. Comparative studies of the properties of CdS films deposited on different substrates by R. F. sputtering [J], *Thin Solid Films*, 2006, 511 - 512: 299 - 303.
- [7] Gupta A, Compaan A D. All-sputtered 14% CdS/CdTe thin-film solar cell with ZnO:Al transparent conducting oxide [J], *Applied Physics Letters*, 2004, 85(4): 684 - 686.
- [8] Roh J S, Im H B. Effects of CdCl<sub>2</sub> in CdTe on the properties of sintered CdS/CdTe solar cells [J], *Journal of Materials Science*, 1988, 23(6): 2267 - 2272.
- [9] Wang S. *Fundamentals of semiconductor theory and device physics* [M], Prentice-Hall, New York, 1989: 222.
- [10] Pankove J I. *Optical process in semiconductors, solid state physical electronic* [M], Prentice-Hall, NJ 1971: 422.
- [1] Tsuji M, Aramoto T, Ohyama H, *et al.* Characterization of CdS thin film in high efficient CdS/CdTe solar cells [J].
- 
- (上接 293 页)
- [4] Ge J, Wu Y H, Zhang C J, *et al.* Comparative study of the influence of two distinct sulfurization ramping rates on the properties of Cu<sub>2</sub>ZnSnS<sub>4</sub> thin films [J]. *Appl. Surf. Sci.*, 2012, 258(19): 7250 - 7254.
- [5] Guo Q J, Ford G M, Yang W C, *et al.* Fabrication of 7.2% Efficient CZTSSe Solar Cells Using CZTS Nanocrystals [J]. *J. Am. Chem. Soc.*, 2010, 132(49): 17384 - 17386.
- [6] Scragg J J, Berg D M, Dale P J. A 3.2% efficient Kesterite device from electrodeposited stacked elemental layers [J]. *J. Electroanal. Chem.*, 2010, 646(1-2): 52 - 59.
- [7] Li J, Ma T T, Wei M, *et al.* The Cu<sub>2</sub>ZnSnSe<sub>4</sub> thin films solar cells synthesized by electrodeposition route [J]. *Appl. Surf. Sci.*, 2012, 258(17): 6261 - 6265.
- [8] Araki H, Kubo Y, Jimbo K, *et al.* Preparation of Cu<sub>2</sub>ZnSnS<sub>4</sub> thin films by sulfurization of co-electroplated Cu-Zn-Sn precursors [J]. *Phys. Status Solidi A*, 2009, 6(5): 1266 - 1268.
- [9] Pawar S M, Pawar B S, Moholkar A V, *et al.* Single step electrosynthesis of Cu<sub>2</sub>ZnSnS<sub>4</sub> (CZTS) thin films for solar cell application [J]. *Electrochim. Acta*, 2010, 55(12): 4057 - 4061.
- [10] Pawar B S, Pawar S M, Shin S W, *et al.* Effect of complexing agent on the properties of electrochemically deposited Cu<sub>2</sub>ZnSnS<sub>4</sub> (CZTS) thin films [J]. *Appl. Surf. Sci.*, 2010, 257(5): 1786 - 1791.
- [11] Ge J, Zuo S H, Jiang J C, *et al.* Investigation of Se supply for the growth of Cu<sub>2</sub>ZnSn(S<sub>x</sub>Se<sub>1-x</sub>)<sub>4</sub> (x ≈ 0.02 ~ 0.05) thin films for photovoltaics [J]. *Appl. Surf. Sci.*, 2012, 258(20): 7844 - 7848.
- [12] Babu G S, Kumar Y B K, Reddy Y B K, *et al.* Growth and characterization of Cu<sub>2</sub>SnSe<sub>3</sub> thin films [J]. *Mater. Chem. Phys.*, 2006, 96(2-3): 442 - 446.
- [13] Altosaar M, Raudoja J, Timmo K, *et al.* Cu<sub>2</sub>Zn<sub>1-x</sub>Cd<sub>x</sub>Sn(S<sub>1-y</sub>S<sub>y</sub>)<sub>4</sub> solid solutions as absorber materials for solar cells [J]. *Phys. Status Solidi A*, 2008, 205(1): 167 - 170.
- [14] Volobujeva O, Raudoja J, Mellikov E, *et al.* Cu<sub>2</sub>ZnSnSe<sub>4</sub> films by selenization of Sn - Zn - Cu sequential films [J]. *J. Phys. Chem. Solids*, 2009, 70(3-4): 567 - 570.
- [15] Chung C H, Li S H, Lei B, *et al.* Identification of the molecular precursors for hydrazine solution processed CuIn(Se,S)<sub>2</sub> films and their interactions [J]. *Chem. Mater.*, 2011, 23(4): 964 - 969.
- [16] Devika M, Reddy N K, Ramesh K, *et al.* Weak rectifying behaviour of p-SnS/n-ITO heterojunctions [J]. *Solid-State Electron.*, 2009, 53(6): 630 - 634.